Journal Pre-proofs

Original article

Widespread applicability of bacterial cellulose-ZnO-MWCNT hybrid membranes

Bilal El Mrabate, Emma Szőri-Dorogházi, Mohammed Ahmed Shehab, Tanya Chauhan, Gábor Muránszky, Emőke Sikora, Ádám Filep, Nikita Sharma, Lilla Nánai, Klara Hernadi, Zoltán Németh

Please cite this article as: B. El Mrabate, E. Szőri-Dorogházi, M. Ahmed Shehab, T. Chauhan, G. Muránszky, E. Sikora, A. Filep, N. Sharma, L. Nánai, K. Hernadi, Z. Németh, Widespread applicability of bacterial cellulose-ZnO-MWCNT hybrid membranes, *Arabian Journal of Chemistry* (2021), doi: https://doi.org/10.1016/j.arabjc.2021.103232

Widespread applicability of bacterial cellulose-ZnO-MWCNT hybrid membranes

Bilal El Mrabate[1,2], Emma Szőri-Dorogházi[1], Mohammed Ahmed Shehab[1,3], Tanya Chauhan[1], Gábor Muránszky[2], Emőke Sikora[2], Ádám Filep[1], Nikita Sharma[1,5], Lilla Nánai[5], Klara Hernadi[4,5], Zoltán Németh[1*]

[1]Advanced Materials and Intelligent Technologies Higher Education and Industrial Cooperation Centre, University of Miskolc, H-3515 Miskolc, Hungary
[2]Institute of Chemistry, University of Miskolc, H-3515 Miskolc, Hungary
[3]Polymers and Petrochemicals Engineering Department, Basrah University for Oil and Gas, 61004 Basrah, Iraq
[4]Institute of Physical Metallurgy, Metal Forming and Nanotechnology, University of Miskolc, 3515 Miskolc-Egyetemváros, Hungary
[5]Department of Applied and Environmental Chemistry, University of Szeged, H-6720, Szeged, Hungary

Abstract

The novel photoactive membranes have grabbed the attention in the field of environmental protection by employing wastewater treatments and the removal of microorganisms or organic pollutants from wastewater. Here we present a promising self-supported photoactive hybrid membrane for future antimicrobial and water treatment applications. In this study, the efficiency of bacterial cellulose (BC) - zinc oxide (ZnO) - multi walled carbon nanotube (MWCNT) hybrid membranes in the adsorption and photocatalytic degradation of methylene blue (MB) under UV radiation and the removal of *Escherichia coli (E. Coli)* was investigated. It was found that the photocatalytic efficiency is strongly dependent on both the preparation method and the amount of ZnO-MWCNT additives loaded into the hybrid membranes. The characterization of BC-ZnO-MWCNT membranes was done using scanning electron microscopy (SEM), mercury intrusion porosimetry (MIP), and X-ray micro computed tomography (μ CT) to study the morphological and porosity aspect of the prepared-membranes. The promising results of this study could provide a new pathway in the field of photocatalysed-based water treatment technology by the application of hybrid membranes.
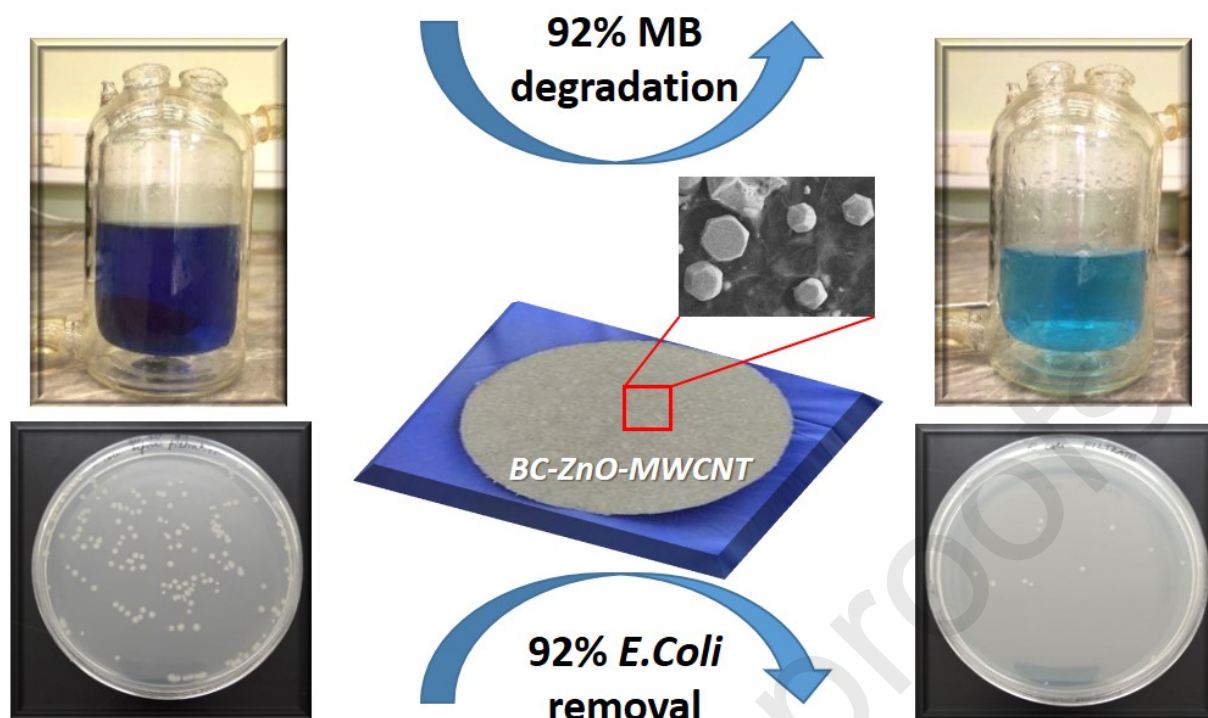
Keywords: hybrid membrane, ZnO-MWCNT composites, micro CT, adsorption, photocatalysis

*Corresponding author. Tel/Fax.:+36 46 565 111/1380. E-mail: kemnemet@uni-miskolc.hu (Zoltan Nemeth) ORCID iD: 0000-0001-7871-3818

1. Introduction

The foremost challenge that mankind is facing currently is to provide healthy drinking water all over the world. The presence of organic dyes and bacteria in drinking water is considered among hazardous class of contaminants that causes health problems and outbreaks of diseases [J.R. Chueca et al., 2017]. As it is well-known, MB is an aggressive dye even at low concentration and is associated with various severe health issues [F. Güzel et al., 2017], while *E. Coli* is a member of the *Gram-negative* bacteria family that can cause gastrointestinal problems and increase the severity of inflammation [K.J. Rao, S. Paria, 2017].

For the eco-friendly and sustainable water supply, the filtration of contaminated water by the removal and degradation of organic dyes and bacteria with photocatalytic hybrid membranes is widely investigated. In this regard, advanced nanomaterials and membrane-based materials for high-efficiency water treatment have received significant attention worldwide. Recently, the

combination of fibrous materials such as MWCNT [A. S. Brady-Estévez et al., 2010] and cellulose [H. Sehaqui et al., 2017] with metal and metal oxide (nano)particles resulted in composites and hybrid structure, which showed promising results in the field of water treatment technology [Y. D. Dong et al., 2021]. Moreover, the design of photocatalytic membrane materials could offer an eco-friendly, sustainable alternative not only for the removal but also the decomposition of contaminations [H. Zhang et al., 2006].

ZnO is a notable semiconductor with a band gap of 3.37 eV and high excitation binding energy (60 meV) at room temperature [Y. Sun et al., 2011]. ZnO particles have three significant advantages for photocatalytic reactions: high optical activity, stability, and high sensitivity for UV-vis light [K.R. Lee et al., 2003]. As a semiconductor in hybrid membranes and composites, ZnO has become one of the most commonly used material, not only to remove and decompose the organic compounds from wastewater using UV irradiation, [V. N. An et al., 2020] but also for antibacterial applications [A. Mocanu et al., 2019] or in real time monitoring of toxic pollutants [J. Yu et al., 2020]. Therefore, combination of ZnO with fibrous support materials, such as bacterial cellulose [Y. D. Dong et al., 2021] or MWCNT could improve the adsorption and photocatalytic efficiency of the whole membrane system [L.P. Zhu et al., 2009].

Several studies presented the preparation of ZnO-MWCNT nanocomposites using various synthesis methods such as impregnation [L. Jiang, L. Gao, 2005], chemical vapour deposition [H. Kim, W. Sigmund, 2002], hydrothermal method [Y. W. Koh et al., 2004] or a novel screen-printed method [R. A. Zargar et al., 2020] and the photocatalytic performance of the as-prepared nanocomposites in the decomposition reaction of organic dyes was determined. Chen et al. presented the photocatalytic activity of ZnO-MWNT nanocomposite for methyl orange (MO) degradation, which is attributed to the excellent electronic property of MWNT and the photocatalytic activity of ZnO under UV irradiation [C. S. Chen et al., 2013]. Li et al. have developed a hybrid film contained ZnO nanorods and ZnO-Zn heterogeneous structure

embedded in carbon nanotubes network and the catalytic property of hybrid film in degrading MB in water was studied [S. Li et al., 2013]. In our previous study, we have also presented a simple route to produce ZnO coated MWCNT composites through the impregnation process. Furthermore, the photocatalytic efficiencies of as-prepared ZnO-MWCNT composites were tested in the decomposition reactions of acetaldehyde (AA) [E. Bartfai et al., 2019].

Nanofibrous cellulose, named as bacterial cellulose (BC), has outstanding properties - e.g. high crystallinity, excellent tensile strength and high modulus [J. Wang et al., 2019] - which makes the BC as promising candidates for developing self-supported hybrid membranes for enhanced removal ability in the area of environmental water remediation or industrial wastewater treatment [A. A. Alves et al., 2020]. Although BC has many excellent properties, there are some drawbacks, which can hinder its widespread utilization. The pure BC does not possess any kind of antibacterial activity [H. Ullah et al., 2016] and has negligible photocatalytic activity under UV or visible light irradiation. However, due to the hydroxyl groups on the surface of the BC, it is an ideal candidate for photoactive nanomaterials as a charge carrier, such as ZnO [F. Fu et al., 2015] or TiO_2 [L. Yang et al., 2020]. Numerous studies demonstrate the preparation and characterization of BC-ZnO nanocomposite materials [M.L. Foresti et al., 2017, N. Janpetch et al., 2016, C. Katepetch et al., 2013] and their utilization in water treatment [M. A. Mohamed et al., 2017] and antimicrobial researches [F. Shahmohammadi et al., 2016]. Furthermore, Wahid et al. used ZnO-BC composite photocatalysts to improve the degradation rate of organic pollutants applying MO as a model pollutant, and the results revealed 91% degradation of MO under UV-irradiation [F. Wahid et al., 2019].

Although many papers showed the preparation and application of BC with various types of metal oxide nanoparticles, there are still some limitations of these membranes such as the vulnerability of the membranes under UV irradiation. In order to extend the lifetime of such

membranes, apart from improving their adsorption and photocatalytic properties, the simultaneous application of BC with two different metal oxides or metal oxide-MWCNT nanocomposites could offer a promising alternative. For instance, Siddiqui et al. reported BC-Fe_2O_3-ZrO_2 [S. I. Siddiqui, S. A. Chaudhry, 2019] and BC-Fe_2O_3-SnO_2 [S. I. Siddiqui et al., 2019] nanocomposites and applied for adsorptive removal of organic dyes and antipathogenic agents from contaminated water.

The photocatalytic performance of hybrid membranes can be improved by controlling the particle size and morphology [K. Rajeshwar et al., 2015]. As numerous studies presented, nanoparticles can cause health problems [P. H. M. Hoet et al., 2004] when they enter the lungs, consequently the regulation of particle size during the design of hybrid membranes could be a critical aspect. By creating a connection between the photocatalytic particles with the use of conducting fibrous materials as channels - e.g. MWCNT - increased adsorption capacity and photoactivity could be obtained due to the more efficient electron transport. Recently, our group showed facile preparations and a wide range of characterization of various self-supported and flexible BC-ZnO-MWCNT hybrid membranes applying impregnation technique and solvothermal method during the preparation of ZnO-MWCNT composites additives [B. El Mrabate et al., 2020]. Results revealed that bacterial cellulose is an ideal carrier to embed the ZnO-MWCNT composites and contributed to the creation of self-supported membranes.

Applying ZnO-MWCNT additives prepared with different synthesis routes in a wide concentration range, the particle size of ZnO, the surface morphology of BC can be tailored easily that are designed to enhance the membrane performance for adsorptive removal of organic dyes and bacteria. Considering the photocatalytic properties of ZnO, the aim of this study is to present the adsorption properties and photocatalytic performance of BC-ZnO-MWCNT hybrid membranes against MB, which showed up to 90% decomposition of adsorbed MB dye. Furthermore, the antibacterial properties of the as-prepared hybrid membranes were

also tested against E. Coli. To our best knowledge, this is the first work that studies the adsorption and photocatalytic properties of BC-ZnO-MWCNT hybrid membranes.
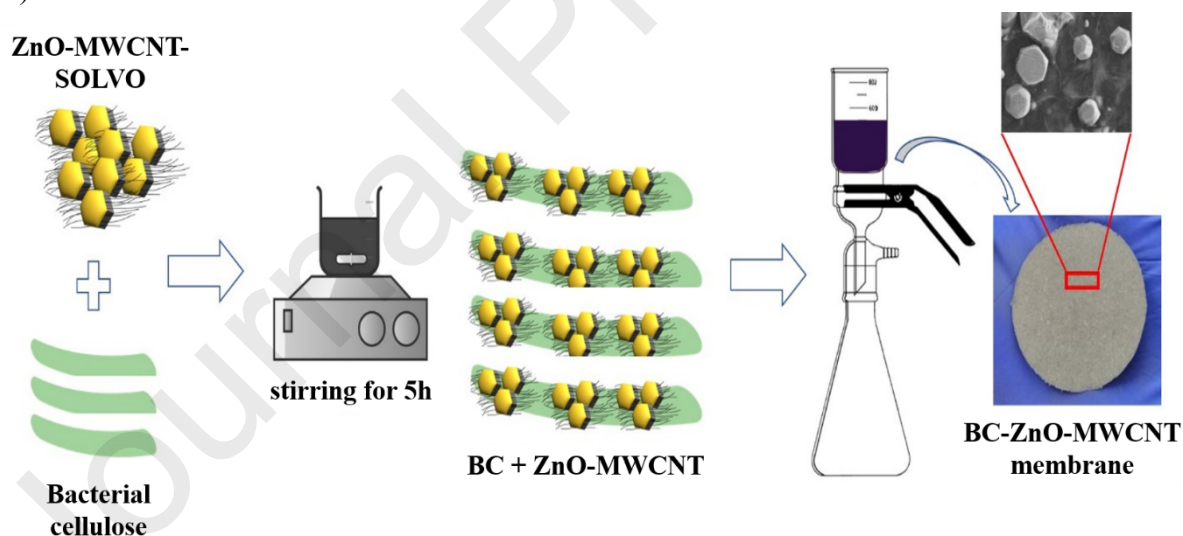
2. Experimental

2.1. Materials

Commercialized MWCNT (NC7000), was purchased from Nanocyl SA, Belgium (with an average diameter of 30 nm, a length of 1.5 μm, and a surface area of 300 m^2/g). Zinc acetate [$Zn(CH_3COO)_2 \times 2H_2O$] (ZnAc) was applied as a precursor compound, the solvent used was absolute ethanol (EtOH), cetyltrimethylammonium bromide (CTAB) was used as surfactant, and methylene blue (MB organic dye) was applied as model pollutant. ZnAc, EtOH, CTAB and MB were purchased from VWR Chemicals, Hungary. MilliQ water (18.2 MΩcm) was used throughout the experiments. BC fibres were received from nata de coco cubes (FI, Philippines) by an alkaline and oxidative purification and a mechanical disintegrate [S. Gea et al., 2011]. For membrane preparation, the BC suspension - dry solid content of 1.0 % - was used. Polytetrafluoroethylene (PTFE) filter of the pore size of 0.22 μm and the diameter of 47 mm (Durapore-GVWP04700) was applied for membrane preparation. Escherichia coli DH5α (Gram-negative) strain was used for filtration test as a model organism.

2.2. Preparation of BC-ZnO-MWCNT hybrid membranes

In our earlier papers, the preparation and investigation of ZnO-MWCNT additives [E. Bartfai et al., 2019, B. El Mrabate et al. 2019]. were shown. In brief, impregnation and solvothermal methods were used to produce the inorganic composite as additives. In all cases, the CTAB modified MWCNT content was adjusted at 10 w/w % of the as-prepared composite materials. Resulted composites were named ZnO-MWCNT-IMP and ZnO-MWCNT-SOLVO depending on the production method.

Recently, we have also presented the preparation of the BC-ZnO-MWCNT hybrid membranes [B. El Mrabate et al., 2020]. During the synthesis of the BC-ZnO-MWCNT membrane materials, the calculated amount of BC was dipped into 15 mL EtOH, while, both of the composite additives (ZnO-MWCNT-IMP and ZnO-MWCNT-SOLVO) were sonicated in 50 mL EtOH for 20 min. The amount of the ZnO-MWCNT composite additives in the hybrid membranes was adjusted to 50 w/w% and 80 w/w %, respectively. In the next step, the BC suspension was mixed to the ZnO-MWCNT-IMP and the ZnO-MWCNT-SOLVO additives and stirred for 5 hours at 300 rpm. Finally, the preparation of BC-based hybrid membranes was accomplished by vacuum filtration through a PTFE membrane to achieve a loading of 8 mg/cm^2 (total mass 100 mg/membrane), then it was dried in air (Fig. 1). Resulted membranes were named as IMP 50 an IMP 80 and SOLVO 50, SOLVO 80, depending on the synthesis route (IMP, SOLVO) and the amount of ZnO-MWCNT composite additive (50 w/w % and 80 w/w %).

Fig. 1. Preparation route of BC-ZnO-MWCNT hybrid membranes.

2.3. Adsorption and photocatalytic experiments

The adsorption capacity and photocatalytic efficiency of the prepared membranes were determined by measuring the degradation of MB as model pollutant in an aqueous solution under UV light ($\lambda_{max} \approx 365$ nm) irradiation. In the adsorption experiment, a given amount of adsorbent is immersed into the MB solution of known volume and concentration. Equilibration was aided by shaking for 2h. The absorbance of methylene blue in the particle-free calibration and sample solutions was determined using a Carl Zeiss Jena Spekol 11 UV-VIS spectrophotometer at 609 nm wavelength. The calibration standards in the concentration range of 0.0025 mM - 0.05 mM were diluted from 1.0 mM concentration stock solution of MB.

The photocatalytic test was carried out in a double-walled Pyrex® glass reactor, as shown in Fig. 2 A, surrounded by a thermostatic jacket (T = 25°C) with water as the thermostatic agent. The reactor was equipped with 6×6 W black light lamps to measure the photocatalytic activity of the synthesized hybrid-membranes, shown in Fig. 2 B. The following important parameters were adopted for the test: initial concentration of MB used for the analysis (C_0 (MB)) = 0.05mM and the total volume of the solution (containing MB) was 100 mL. The reactor was continuously purged with air in order to keep the concentration of dissolved oxygen constant throughout the experiment. The solution, with the membrane inside, was kept under dark for two hours to attain the adsorption-desorption equilibrium.

This was followed by UV light irradiation for another two hours, therefore, total irradiation time was two hours. Approximately 1.5 mL of the samples were withdrawn at different time intervals and centrifuged for 3 min at 13,400 rpm and filtered with Filtratech 0.25 μm syringe filter. For the first hour, the samples were taken in every 10 minutes. After this, the samples were taken after every 20 minutes. The concentration of MB was followed by using a P4 VWR UV-Vis spectrophotometer with maximum absorption wavelength (λmax) = 664 nm. The degradation percentages of MB in aqueous solution was calculated as follows:

$$\text{Degradation (\%)} = (C_0 - C_t)/C_0 \times 100$$

where, C_0 = initial concentration at time t = 0, and C_t = concentration at time interval "t".
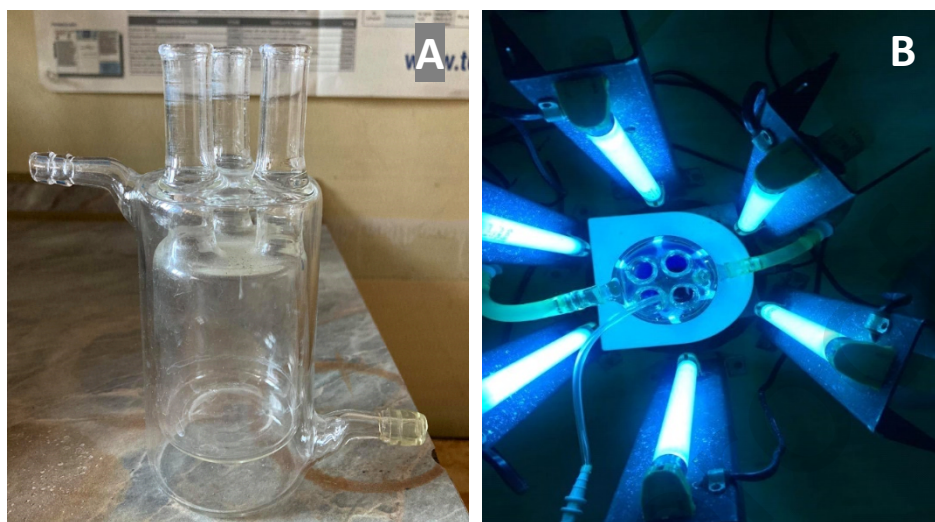
Fig. 2. Photocatalytic reactor used for the study (A); assembly of the whole reactor system with UV lamps (B).

2.4. Bacterial filtration efficiency (BFE) test

For bacterial filtration efficiency test, ten-fold serial dilution was made from the initial starter culture in 30 mL Lysogeny Broth (LB) medium. The colony forming unit (cfu) concentration of the sixth ten-fold dilution was $1.50 \pm 0.20 \times 103$ cfu/mL determined by the colony counting method. This suspension was used for the filtration experiment providing a countable number of colonies on the agar plate. Before each filtration, 3×100 µL sample was evenly spread on the top of LB agar plate to check the initial colony forming unit concentration (CFU0). The filtration was performed using glass vacuum filtration device (Sartorius Stedim Biotech 16306 - 25 mm) attached to a vacuum pump (Millipore) and the suction force of the vacuum pump was adapted in such a way that the flow rate of the suspension through the filter remained the same for each experiment (0.8 bar). After filtration 3×100 µL sample was also

taken from the filtrated suspension to determine the number of the colony forming units of the filtrate (CFUf) and then to derive BFE% values using the following formula:

$$BFE\% = \frac{CFU_0 - CFU_f}{CFU_0} \cdot 100\%$$

2.5. Characterization

The surface morphology of hybrid membranes before and after filtration experiments was investigated by scanning electron microscopy (SEM) and focus ion beam scanning electron microscopy (FIB-SEM). SEM investigation was performed with the use of Hitachi S-4700 Type II FE-SEM operating in the range of 0-30 keV. FIB-SEM measurements were done with a Thermo Helios G4 PFIB CXe instrument. Moreover, the three-dimensional architecture of the hybrid membranes was characterized using YXLON FF35 dual-beam X-ray micro computed tomography equipment (CT) (microfocus X-ray tube, transmission beam, acceleration voltage: 50 kV).

Hybrid membranes were also investigated by mercury intrusion porosimetry (MIP) to determine the pore size distribution. Measurements were done on PASCAL 140 (low pressurization system down to 0.04 MPa) and PASCAL 440 (high pressurization system up to 400 MPa) instruments (manufactured by Thermo Scientific).

The absorbance of MB in the calibration and sample solutions was determined using a Carl Zeiss Jena Spekol 11 UV-VIS spectrophotometer at 609 nm wavelength. The concentration of MB during the photocatalytic experiments was followed by using a P4 VWR UV-Vis spectrophotometer with maximum absorption wavelength ($\lambda_{max} = 664$ nm).

Furthermore, our previous study presented a wide range of characterization of the as-prepared membranes with the use of X-ray powder diffraction (XRD), specific surface area measurement (BET), Raman microscopy investigation, electrophoretic measurement (dynamic light scattering - DLS), contact angle measurement, and mechanical tests [35].

3. Results and discussion

3.1 SEM and CT analysis

The morphology of neat BC membrane (Fig. 3 A) and the surface structure of as-prepared BC-ZnO-MWCNT hybrid membranes (Fig. 3 B-C and Fig. 4) was characterized by SEM (Fig. 3) and CT (Fig. 4) techniques. Flexible hybrid membranes were produced successfully in each case, although a significant difference was observed during the SEM analysis, as we presented recently [B. El Mrabate et al., 2020]. Due to the formation of interfacial bonds between the hydroxyl (–OH) groups on BC and the oxygen-containing species on the surface of MWCNT stable and self-supported membranes can be gained with both synthesis methods [H. Qi et al., 2014].

Fig. 3 B clearly demonstrates the presence of presumably ZnO nanoparticles (averagely 20-30 nm) and bigger ZnO agglomerates on the surface of BC fibres prepared by the impregnation method. Using ZnO-MWCNT-SOLVO additive (Fig. 3 C), the as-prepared membranes consist of hexagonal ZnO particles with an average size of 4-5 μm, and as we described, the MWCNT was built into ZnO crystals [B. El Mrabate et al., 2020]. In this paper energy dispersive X-ray spectroscopy (EDAX) analysis was also performed for each sample to identify the composition of the as-prepared hybrid membranes. These investigations confirmed the carbon (C), oxygen (O) and zinc (Zn) signals, which are originating from the MWCNT, BC and ZnO [B. El Mrabate et al., 2020].
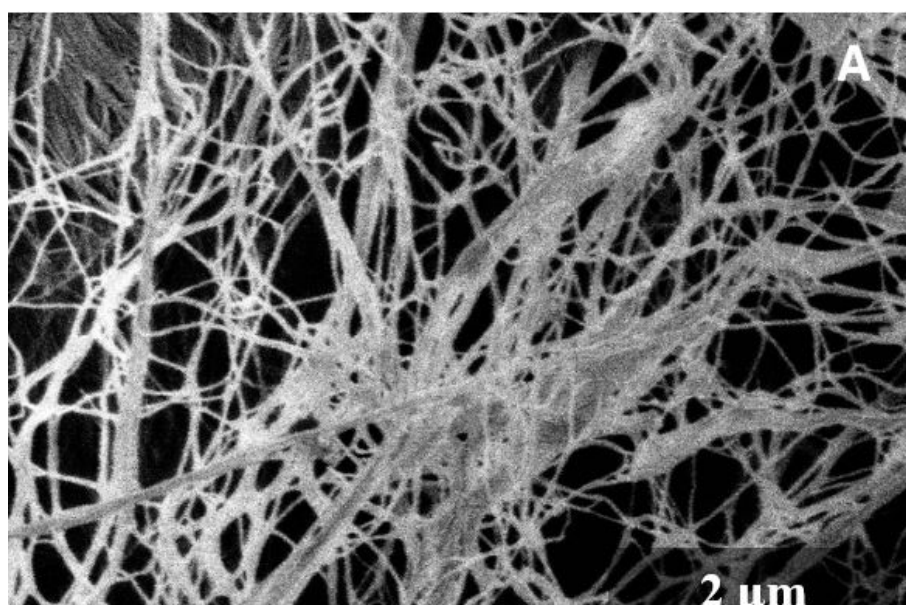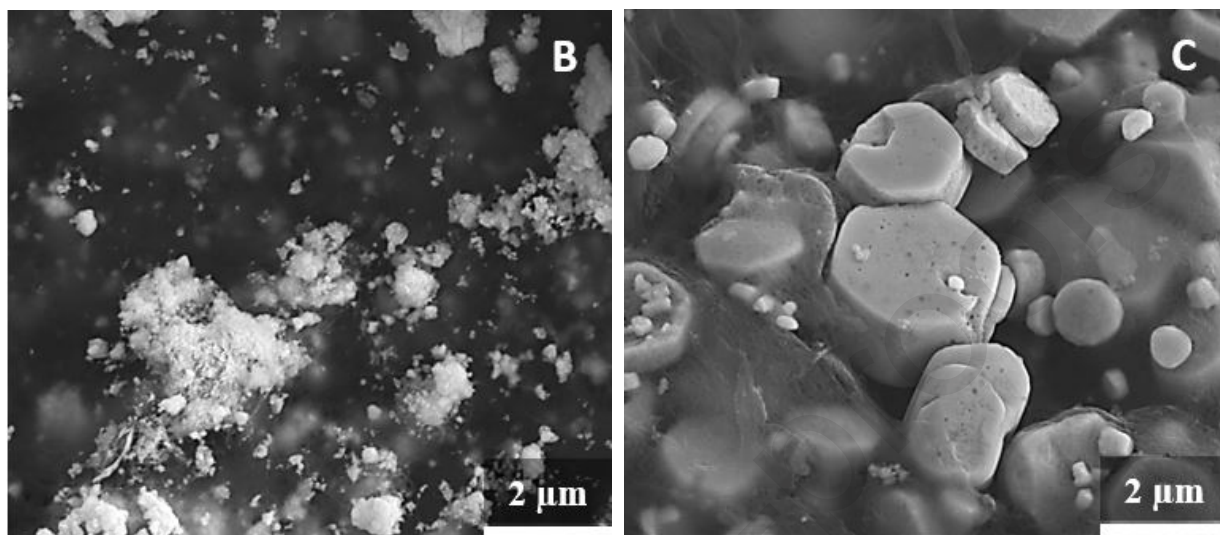
Fig. 3. SEM micrographs of neat BC membrane (A) and BC-ZnO-MWCNT hybrid membranes prepared by impregnation technique (IMP 50 - B) and solvothermal method (SOLVO 50 - C).

Although, the electron microscopy is often used during the analysis of nanocomposite materials, there are some limitations of these techniques - e.g. the size of the investigated area. In order to gain information about the homogeneity and the surface morphology of the whole membrane, CT analysis was performed in the case of SOLVO membranes. Fig. 4 A shows the cross section analysis, while Fig. 4 B shows the surface morphology of SOLVO 50 membrane. The bright dots in Fig. 4 B and C represent the homogeneous distribution of ZnO microcrystals on the surface of the hybrid membrane. The volume of the individual ZnO particles was also determined in the full 3D extension of the sample (Fig. 4 C). It was found that 95 % of the ZnO microparticles have a volume from $5{\times}10^{-8}$ mm^3 to $1.16{\times}10^{-6}$ mm^3 in the case of both types of SOLVO membranes (Fig. 4 D). Presumably, these ZnO microcrystals could play an important role in the photocatalytic decomposition of organic dyes and/or bacteria as larger photoactive

centres. It is clear that ZnO particles in the micrometer range have significantly higher volume than ZnO nanoparticles, consequently, increased photocatalytic performance can be assumed by applying SOLVO membranes.
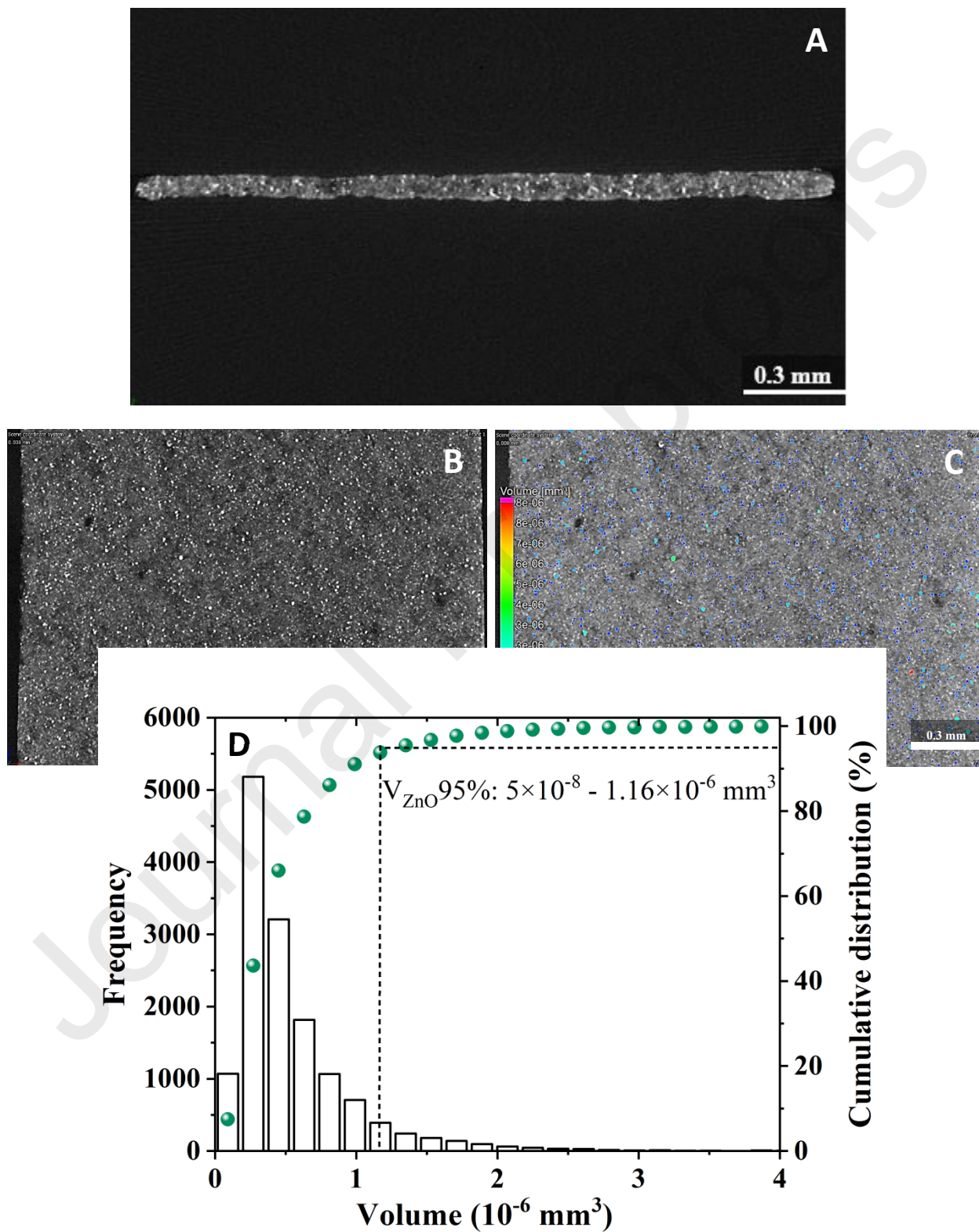
Fig. 4. CT analysis of SOLVO 50 hybrid membrane: cross section analysis (A); surface morphology (B), particle volume distribution (C and D).

3.2 Pore size distribution (PSD) analysis

According to the relative pore volume histograms (Fig. 5), the membranes prepared by the impregnation technique has a wider pore size distribution range. As it can be seen in Fig. 5, the majority of pores are in the range of 10 μm to 100 μm in all membranes.
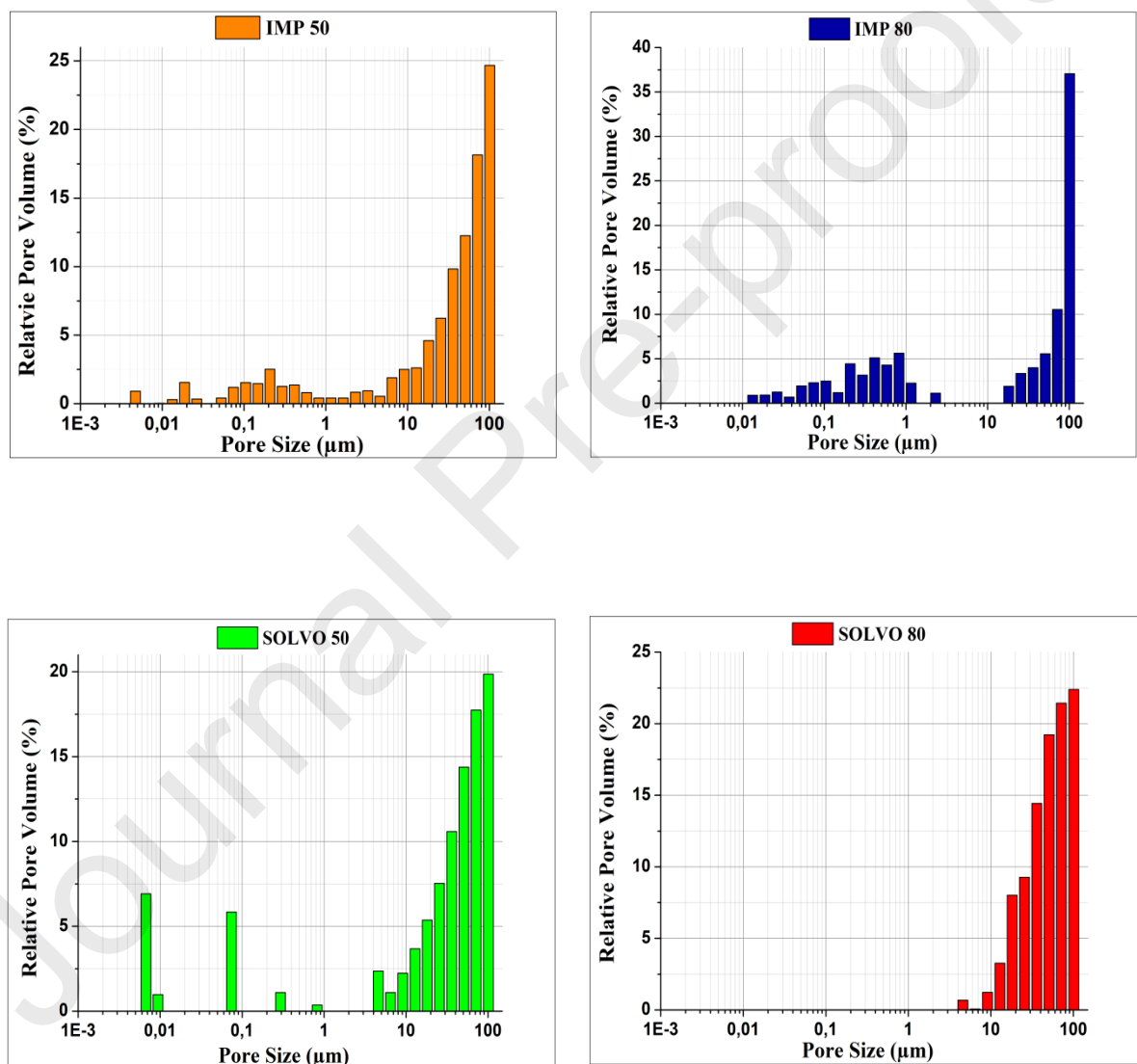
Fig. 5. Pore size distribution analysis of hybrid membranes.

Comparing the hybrid membranes, it can be concluded that the average pore size of SOLVO membranes is significantly higher than that of IMP membranes. The pores that are

larger than 10 μm occupied a cumulative pore volume of about 77.0 % and 97.0 % for SOLVO 50 and SOLVO 80, respectively. Moreover, the SOLVO 80 membrane possesses a relatively narrow PSD with the highest relative pore volume at 98.8 μm, while SOLVO 50 shows a wider PSD with 2 larger peaks at 0.008 μm, and 0.085 μm. In the case of IMP samples, the peaks shifted towards the smallest pores and the number of pores below 10 μm has been increased, in particular those of under 1 μm. Based on the pore size distribution analysis, we assumed that the as-prepared hybrid membranes are suitable for filtration and adsorption experiments.

3.3 Adsorption capacity and photocatalytic decomposition of MB

The Langmuir isotherm models (Fig. 6) were used to describe the equilibrium characteristics of the MB adsorption. The Langmuir is defined by the following equations:

$$q_e = \frac{q_m \times K_L \times c_e}{1 + c_e \times K_L}$$

where q_e is the amount (mmol/g), while c_e is the equilibrium concentration of MB in the solution (mmol/L), q_m is the maximum sorption capacity (mmol/g) and K_L is the Langmuir equilibrium constant (L/mg). K_L and q_m can be calculated with nonlinear regression. The parameters obtained from the fitted isotherms are shown in Table 1. The correlation coefficients (R^2) are close to 1 in both cases, so the isotherms fit well with the results. According to the results, the maximum adsorption capacity (q_m) was higher for IMP 80 (0.040 mmol/g) than for IMP 50 (0.031 mmol/g).
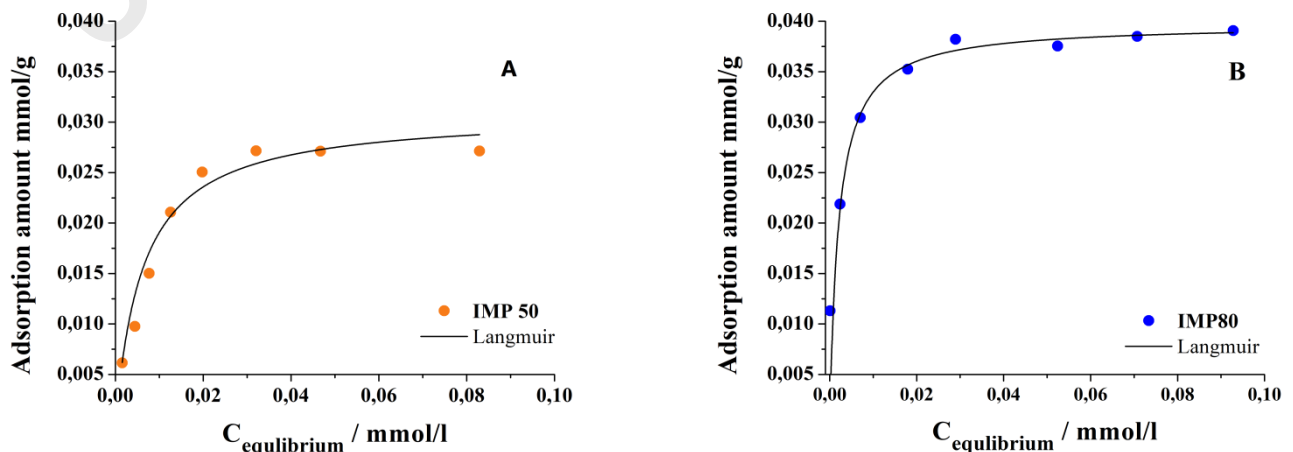
Fig. 6. Adsorption isotherms of IMP 50 (A) and IMP 80 (B) hybrid membranes.

Sample	q_m (mmol/g)	K_L (L/mg)	R^2
IMP 50	0.031 ± 0.001	160.8 ± 35	0.9982
IMP 80	0.040 ± 0.0004	488.6 ± 63	0.9997

Table 1 The calculated Langmuir adsorption parameters.

For studying the photocatalytic degradation performance of the membranes prepared by two different methods, MB was used as a targeted pollutant to support the photodegradation efficiency of the prepared membranes. The highest degradation was achieved by the membrane SOLVO 80 with a removal efficiency of 92% after 120 minutes under UV light, as can be seen in Fig. 7 (red curve), followed by 78% decomposition of MB by SOLVO 50 membrane, Fig. 7 (green curve). Furthermore, there was no significant MB decomposition was observed under UV irradiation applying the same experimental setup in the absence of hybrid membrane catalysts, as can be seen in Figure 7 light blue curve.
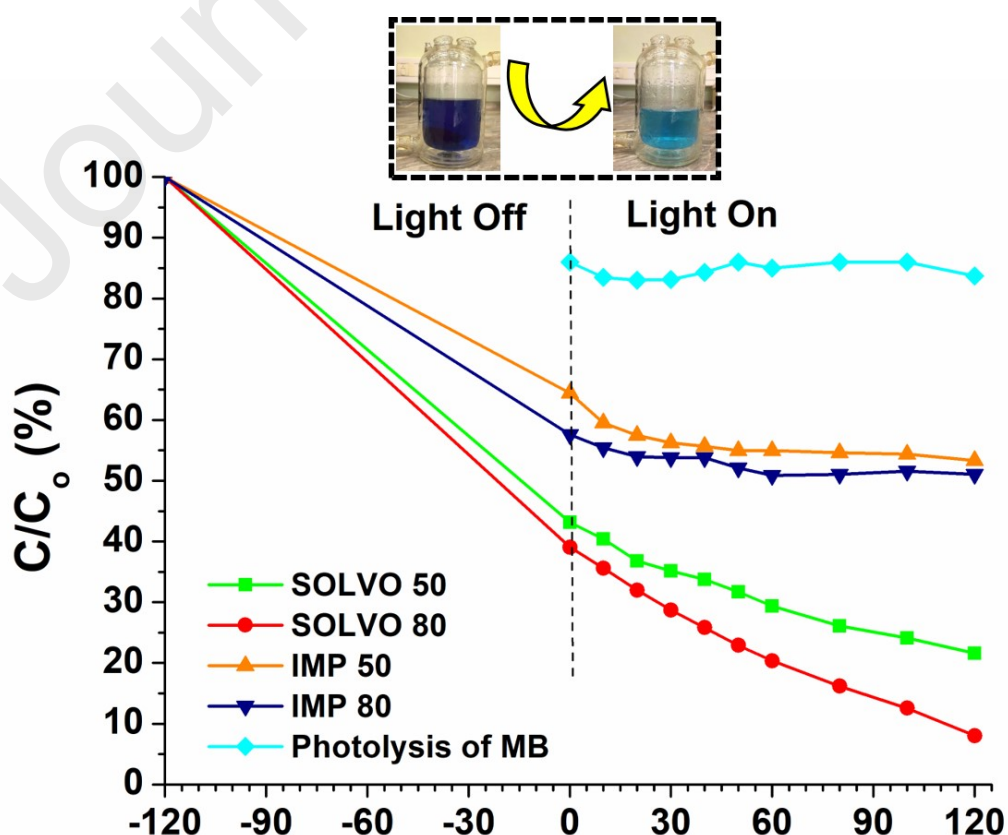
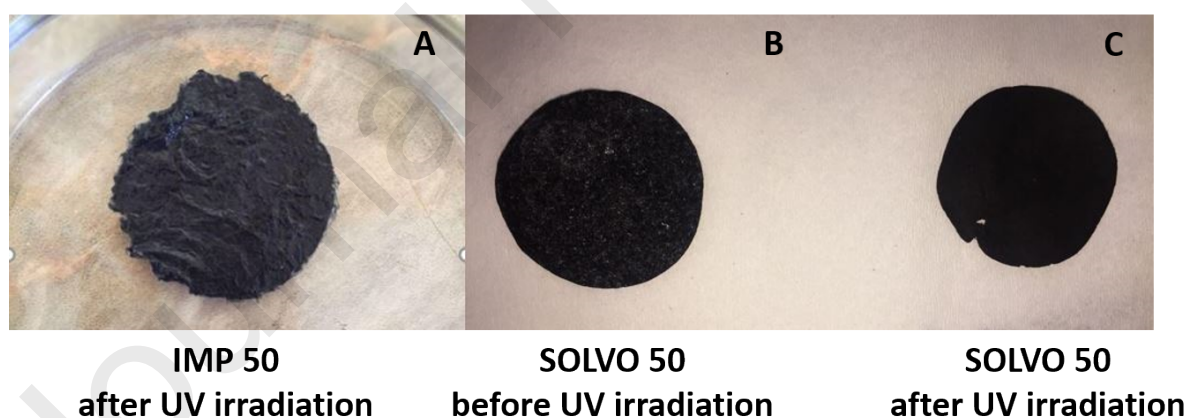**Fig. 7.** Photocatalytic degradation rate of MB over the different hybrid membranes under UV irradiation.

However, the lowest degradation efficiencies were achieved by the membranes prepared *via* impregnation technique with the overall removal efficiency of 47% and 49%, for IMP 50 and IMP 80 (Fig. 7 orange and blue curves), respectively. Apparently, the membranes with higher ZnO-MWCNT content (80%) resulted in higher adsorption capacity for MB. The higher activity of the SOLVO membranes can also be supported by the higher specific surface areas as compared to impregnated membrane version, which was also reported in our previous work [B. El Mrabate et al., 2020]. It means that the solvothermal method resulted in materials with higher removal efficacies compared to the ones prepared *via* impregnation method.

MWCNT is well-known for their high adsorption and good electron acceptor properties [Y. Sun et al., 2001]. Both the MWCNT and bacterial cellulose are possessing remarkable physico-chemical and mechanical properties, which provide superior performance via synergistic effects after combining. Furthermore, the photocatalytic degradation of MB can be explained by the electron transfer process from the ZnO particles to MWCNT [E. Bartfai et al., 2019]. Carbon nanotubes acts as a photogenerated electron acceptor to promote interfacial electron transfer processes from the ZnO particles to the MWCNT. Moreover, the bacterial cellulose, in addition, has hydroxyl groups in abundance on its surface, which may also act as a charge carrier further improving the catalytic performance of the hybrid membranes.

The enhanced photocatalytic activity of BC-ZnO-MWCNT SOLVO membranes denotes that a good interfacial combination exists between ZnO nanoparticles and the MWCNT in the

as-prepared composites [P. Berki et al., 2013]. Although, the better photocatalytic performance of SOLVO membranes could be explained not only with the chemical bond between the ZnO and MWCNT, but also to the size and volume of ZnO particles. The incorporation of ZnO-MWCNT-SOLVO additives into the BC matrix resulted in increased photoactivity of the hybrid membranes, due to the presence of micrometer sized ZnO particles, which can also be described as the photoactive center of MB degradation. The high removal and adsorption rates of the bacterial cellulose reinforce hybrid membranes prepared *via* solvothermal method indicates good adsorption and photocatalytic activity for MB and is likely to be an efficient photocatalyst.

It was also observed during the experimental process that membranes prepared *via* IMP method were less stable physically (see Fig. 8 A) and started to become deformed after few minutes. Some loose threads-like fibrous part of membranes were also could be observed during sample collection. On the other hand, membranes synthesized by SOLVO method were not deformed and maintained their original physical state throughout the whole experiment (Fig. 8 B and C).

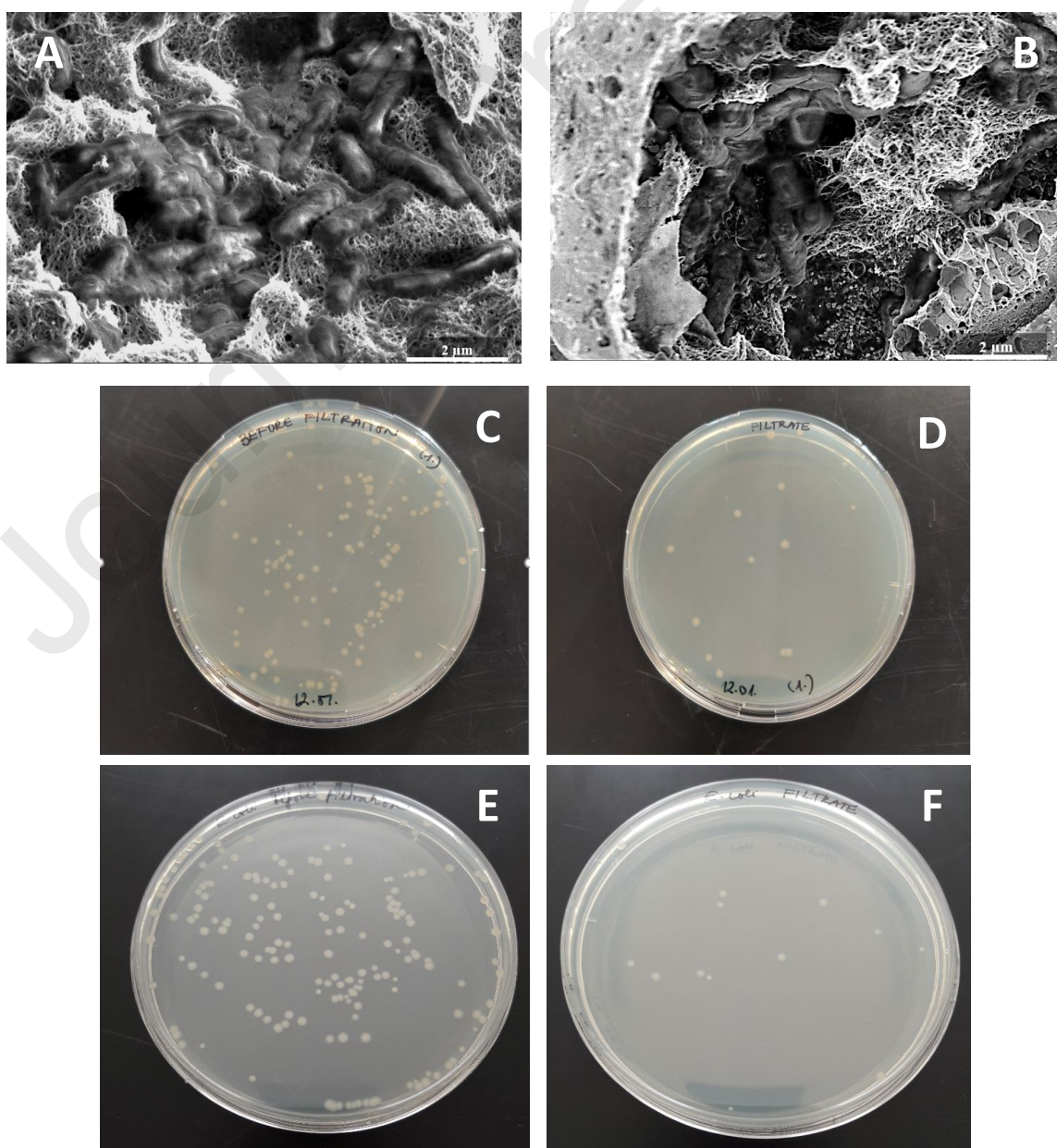| IMP 50 | SOLVO 50 | SOLVO 50 |
| after UV irradiation | before UV irradiation | after UV irradiation |

Fig. 8. Membrane degradation of IMP (A) and SOLVO (B and C) membranes before and after UV irradiation**.**

3.4 E. Coli filtration experiments

Before the filtration tests began, control experiments were performed without applying the as-prepared hybrid membranes to investigate the possible adsorption on the membrane

holder of the funnel. This investigation revealed that there was no measurable *E. Coli* retention. During the first series of the measurement, BC-ZnO-MWCNT-IMP membranes even at 50 w/w% BC content were damaged due to the negative differential pressure. It strongly correlates with our previous published results [B. El Mrabate et al., 2020]. Comparing the membranes, it was found that SOLVO 80 showed significantly higher tensile strength (6.7±1.7 MPa) than IMP 80 (1.1±0.5 MPa). To avoid this phenomenon and to obtain comparative results, two superimposed membranes were applied in each filtration cycle. Applying this experimental setup, we were able to stabilize the membrane structure against the applied pressure (0.8 bar).

Fig. 9. SEM images of IMP 50 (A) and SOLVO 50 (B) membranes after filtration. Photographs of E. Coli cultures before filtration with IMP 80 (C) and SOLVO 80 (E), and after the experiments with IMP 80 (D) and SOLVO 80 (F) membranes.

As can be seen in SEM images (Fig. 9 A and B), the *E. Coli* removal was successful using both IMP (Fig. 9 A) and SOLVO (Fig. 9 B) hybrid membranes. Rod shaped *E. Coli* bacteria could be found in these SEM images with an average length of 2-3 μm. Moreover, it can be also observed that the cell wall of the *E. Coli* bacteria was damaged during the filtration. Thus, we assume that novel BC-MWCNT-ZnO hybrid membranes has not only good adsorption ability against *E. Coli* but also has some antibacterial activity. The antibacterial properties of cellulose/ZnO nanocomposite films [F. Wahid et al., 2019] and the pure carbon nanotubes [M. A. Saleemi et al., 2020] have already presented recently. Consequently, the perceived antibacterial effect can be attributed to the synergistic effect of the ingredients of hybrid membranes and the interactions between them.

In both cases, the membranes containing 80 w/w % of ZnO-MWCNT additives showed significantly higher E. Coli removal than samples prepared using 50 w/w % of additives. Figs. 9 C-F and 10 present the removal efficiency of BC-ZnO-MWCNT hybrid membranes. It was found that the highest *E. Coli* removal was achieved by the membrane SOLVO 80 with an efficiency of 92% (Fig. 9 F and Fig. 10 red column).

IMP 80 membrane showed 91% adsorption of *E. Coli*, as can be seen in Fig. 9 D and Fig. 10 blue column. The lowest bacteria removal capacities were achieved by the membranes containing 50 w/w % ZnO-MWCNT additives with the overall removal efficiency of 71% and

57%, for SOLVO 50 and IMP 50 (Fig. 10 green and orange column), respectively. Based on the above-mentioned results, it was found that in terms of *E. Coli* removal, the amount of ZnO-MWCNT composite material incorporated into the hybrid membrane structures is more important than the size of ZnO particles. As can be seen in Fig. 10 the increased amount of ZnO-MWCNT additive content caused a significant improvement in the E. Coli filtration efficiency in both cases. Consequently, the outstanding filtration performance of IMP 80 and SOLVO 80 membranes indicates that the antibacterial properties of the membranes are mainly attributed to the ZnO-MWCNT additive and not to the bacterial cellulose, as it was expected.
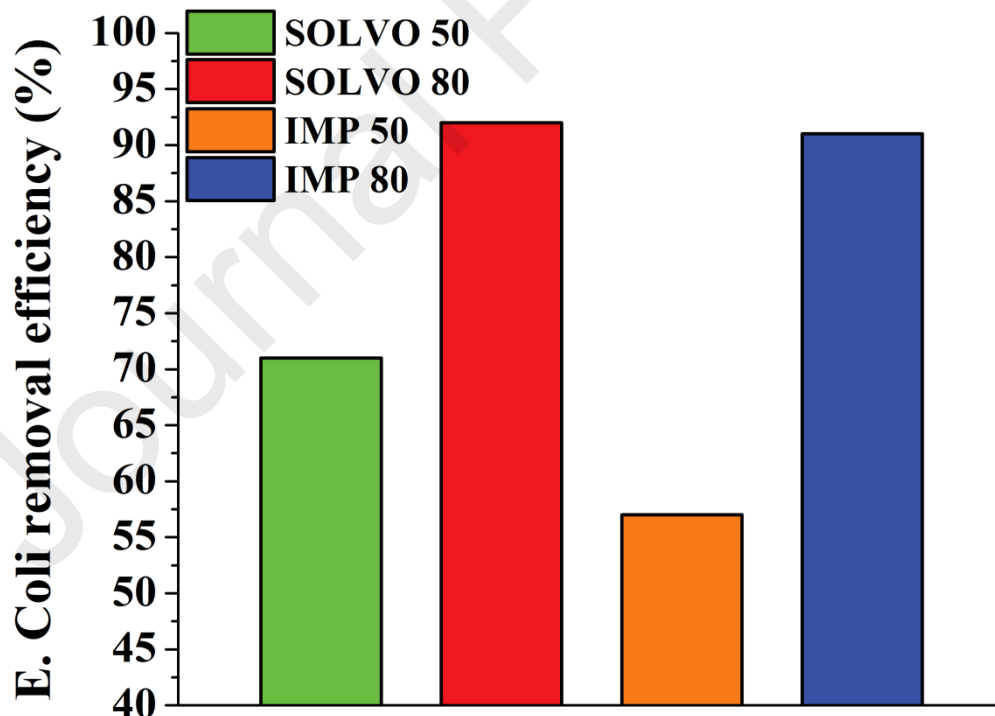

Fig. 10. *E.Coli* removal efficiency (BFE%) of BC-ZnO-MWCNT hybrid membranes.

4. Conclusion

In this study, the development of novel bacterial cellulose-ZnO-MWCNT hybrid membranes and their adsorption, photocatalytic and antibacterial properties were presented. The following hybrid-system of membranes was prepared by two different synthesis techniques, namely, impregnation (IMP) and solvothermal (SOLVO) methods. The as-prepared membranes were characterized by SEM, CT and MIP equipment. Based on the applied preparation method – IMP or SOLVO – a significant difference in the size of ZnO particles was observed. Applying impregnation method, ZnO nanoparticles with an average size of 20-30 nm were formed, while using solvothermal route, micrometer-sized ZnO crystals evolved among the MWCNTs.

The photocatalytic degradation of MB and the removal efficiency and antibacterial properties against *Gram-negative E. Coli* bacteria of the as-prepared hybrid membranes were studied. Comparing the results, it was found that SOLVO 80 membrane showed outstanding properties during these experiments. Both the photocatalytic degradation of MB and the *E. Coli* removal efficiency was achieved 92% in the case of SOLVO 80. Moreover, SOLVO membranes showed much better mechanical stability under UV-irradiation and in the filtration experiments. In contrast, IMP membranes were damaged during both photocatalysis and filtration experiments due to their lower tensile strength parameter. Thus, the application of BC-ZnO-MWCNT-SOLVO membranes containing ZnO particles in a micrometer range could offer further advantages and potential application alternatives such as a field of photocatalyst-based water treatment technology.

References

A. A. Alves, W. E. Silva, M. F. Belian, L. S. G. Lins, A. Galembeck, Bacterial cellulose membranes for environmental water remediation and industrial wastewater treatment, Int. J. Environ. Sci. Tech. 17 (2020) 3997-4008. https://doi.org/10.1007/s13762-020-02746-5

A. Mocanu, G. Isopencu, C. Busuioc, O.M. Popa, P. Dietrich, L. Socaciu-Siebert, Bacterial cellulose films with ZnO nanopartilcles and propolis extracts: synetgistic antimicrobial effect, Sci. Rep. 9 (2019) 17687. https://doi.org/10.1038/s41598-019-54118-w

A. S. Brady-Estévez, M. H. Schnoor, C. D. Vecitis, N. B. Saleh and M. Elimelech, Multiwalled carbon nanotube filter: improving viral removal at low pressure, Langmuir 26 (2010) 14975-14982. https://doi.org/10.1021/la102783v

B. El Mrabate, M. Udayakumar, E. Csiszar, F. Kristaly, M. Lesko, L. Somlyai Sipos, M. Schabikowski, Z. Nemeth, Development of bacterial cellulose-ZnO-MWCNT hybrid membranes: a study of structural and mechanical properties, *R. Soc. Open Sci.* 7 (2020) 200592. https://doi.org/10.1098/rsos.200592

B. El Mrabate, M. Udayakumar, Z. Nemeth, Comparative electron microscopy study of the ZnO/MWCNT nanocomposites prepared by different methods, *Circular Economy Envrion. Protech.* 3(1) (2019) 16-24.

C. Katepetch, R. Rujiravanit, H. Tamura, Formation of nanocrytalline ZnO particles into bacterial cellulose pellicle by ultrasonic-assisted in situ synthesis, Cellulose 20 (3) (2013) 1275-1292. https://doi.org/10.1007/s10570-013-9892-8

C. S. Chen, T.G. Liu, L.W. Lin, X.D. Xie, X.H. Chen, Q. C. Liu, B. Liang, W. W. Yu, C.Y. Qiu, Multi-walled carbon nanotube supported metal-doped ZnO nanoparticles and their photocatalytic activity, J. Nanopart. Res. 15 (2013) 1295. https://doi.org/10.1007/s11051-012-1295-5

E. Bartfai, K. Nemeth, B. El Mrabate, M. Udayakumar, K. Hernadi, Z. Nemeth, Synthesis, characterization and photocatalytic efficiency of ZnO/MWCNT nanocomposites prepared under different solvent conditions, J. Nanosci. Nanotechnol. 19(1) (2019) 422-428. https://doi.org/10.1166/jnn.2019.15773

F. Fu, L. Li, I. Liu, J. Cai, Y. Zhang, Construction of cellulose based ZnO nanocomposite films with antibacterial properties through one-step coagulation, ACS Appl. Mater. Interfaces 7(4) (2015) 2597-2606. https://doi.org/10.1021/am507639b

F. Güzel, H. Saygili, G.A. Saygili, F. Koyuncu, C. Yilmaz, Optimal oxidation with nitric acid of biochar derived from pyrolysis of weeds and its application in removal of hazardous dye methylene blue from aqueous solution, J. Clean. Prod. 144 (2017) 260-265. https://doi.org/10.1016/j.jclepro.2017.01.029

F. Shahmohammadi, Jebel, H. Almasi, Morphological, physical, antimicrobial and release properties of ZnO nanoparticles-loaded bacterial cellulose films, Carbohydr. Polym. 149 (2016) 8-19. https://doi.org/10.1016/j.carbpol.2016.04.089

F. Wahid, Y.X. Duan, X.H. Hu, L.Q. Chu, S.R. Jia, J.D. Cui, C. Zhong, A facile construction of bacterial cellulose/ZnO nanocomposite films and their photocatalytic and antibacterial properties, Inter. J. Biol. Macromol. 132 (2019) 692-700. https://doi.org/10.1016/j.ijbiomac.2019.03.240

H. Kim, W. Sigmund, Zinc oxide nanowires on carbon nanotubes, Appl. Phys. Lett. 81 (2002) 2085-2087. https://doi.org/10.1063/1.1504877

H. Ullah, F. Wahid, H.A. Santos, T. Khan, Advances in biomedical and pharmaceutical applications of functional bacterial cellulose-based nanocomposites, Carbohydr. Polym. 150 (2016) 406-420. https://doi.org/10.1016/j.carbpol.2016.05.029

H. Qi, J. Liu, E. Mäder, Smart cellulose fibers coated with carbon nanotube networks, *Fibers* 2(4) (2014) 295-307. https://doi.org/10.3390/fib2040295

H. Sehaqui, L. Schaufelberger, B. Michen and T. Zimmermann, Humic acid desorption from a positively charged nanocellulose surface, J. Coll. Interface Sci. 504 (2017) 500-506. https://doi.org/10.1016/j.jcis.2017.06.006

H. Zhang, X. Quan, S. Chen, H. Zhao, Y. Zhao, Fabrication of photocatalytic membrane and evaluation its efficiency in removal of organic pollutants from water, Sep. Purif. Technol. 50(2) (2006) 147-155. https://doi.org/10.1016/j.seppur.2005.11.018

J.R. Chueca, S.I. Moreira, M.S. Lucas, J.R. Fernandes, P.B. Tavares, A. Sampaio, J.A. Peres, Disinfection of simulated and real winery wastewater using sulphate radicals: peroxymonosulphate/transition metal/UV-A LED oxidation, J. Clean. Prod. 149 (2017) 805-817. https://doi.org/10.1016/j.jclepro.2017.02.135

J. Yu, M. Yang, Z. Li, C. Liu, Y. Wei, C. Zhang, B. Man, F.Lei. Hierarchical particle in quasicavity architecture for ultratrace in situ raman sensing and its application in real-time monitoring of toxic pollutants, Anal. Chem. 92(21) (2020) 14754-14761. https://doi.org/10.1021/acs.analchem.0c03375

J. Wang, J. Tavakoli, Y. Tang, Bacterial cellulose production, properties and applications with different culture methods - a review. Carbohydr. Polym. 219 (2019) 63-76. https://doi.org/10.1016/j.carbpol.2019.05.008

K.J. Rao, S. Paria, Phytochemicals mediated synthesis of multifunctional $Ag-Au-TiO_2$ heterostructure for photocatalytic and antimicrobial applications, J. Clean. Prod. 165 (2017) 360-368. https://doi.org/10.1016/j.jclepro.2017.07.147

K. Rajeshwar, A. Thomas, C. Janaky, Photocatalytic activity of inorganic semiconductor surfaces: myths, hype, and reality, J. Phys. Chem. Lett. 6(1) (2015) 139-147. https://doi.org/10.1021/jz502586p

K. R. Lee, S. Park, J.H. Lee, Rapid Ag recovery using photocatalytic ZnO nanopowders prepared by solution-combustion method, J. Mat. Sci. Lett. 22 (2003) 65-67. https://doi.org/10.1023/A:1021738526590

L. Jiang, L. Gao, Fabrication and characterization of ZnO-coated multi-walled carbon nanotubes with enhanced photocatalytic activity, Mat. Chem. Phys. 91(2-3) (2005) 313-31. https://doi.org/10.1016/j.matchemphys.2004.11.028

L.P. Zhu, G.H. Lia, W.Y. Huang, L.L. Ma, Y. Yang, Y. Yu, S.Y. Fu, Preparation, characterization and photocatalytic properties of ZnO-coated multi-walled carbon nanotubes, Mat. Sci. Eng. B 163 (3) (2009) 194-198. https://doi.org/10.1016/j.mseb.2009.05.021

L. Yang, C. Chen, Y. Hu, F. Wei, J, Cui, Y. Zhao, X. Xu, X. Chen, D. Sun, Three-dimensional bacterial cellulose/polydopamine/TiO_2 nanocomposite membrane with enhanced adsorption and photocatalytic degradation for dyes under ultraviolet-visible irradiation, J. Coll. Inter. Sci. 562 (2020) 21-28. https://doi.org/10.1016/j.jcis.2019.12.013

M. A. Mohamed, M. A. Mutalib, Z. A. M. Hir, F.M. Zain, A. B. Mohamad, L. J. Minggu, N.A. Awang, W.N.W. Salleh, An overview on cellulose-based material in tailoring bio-hybrid nanostructured photocatalysts for water treatment and renewable energy applications, Int. J. Biol. Macromol. 103 (2017) 1232-1256. https://doi.org/10.1016/j.ijbiomac.2017.05.181

M. A. Saleemi, M. H. Fouladi, P. V. C. Yong, E. H. Wong, Elucidation of antimicrobial activity of non-covalently dispersed carbon nanotubes, Materials 13(7) (2020) 1676. https://doi.org/10.3390/ma13071676

M. L. Foresti, A. Vázquez, B. Boury B, Applications of bacterial cellulose as precursor of carbon and composites with metal oxide, metal sulfide and metal nanoparticles: a review of recent advances, Carbohydr. Polym. 157 (2017) 447-467. https://doi.org/10.1016/j.carbpol.2016.09.008

N. Janpetch, N. Saito, R. Rujiravanit, Fabrication of bacterial cellulose-ZnO composite via solution plasma process for antibacterial applications, Carbohydr. Polym. 148 (2016) 335-344. https://doi.org/10.1016/j.carbpol.2016.04.066

P. Berki, Z. Németh, B. Réti, O. Berkesi, A. Magrez, V. Aroutiounian, L. Forro, K. Hernadi, Preparation and characterization of multiwalled carbon nanotube/In_2O_3 composites, Carbon 60 (2013) 266-272. https://doi.org/10.1016/j.carbon.2013.04.035

P. H. M. Hoet, I. Brüske-Hohlfeld, O. V. Salata, Nanoparticles - known and unknown health risks, J. Nanobiotechnol. 2 (2004) 12. https://doi.org/10.1186/1477-3155-2-12

R. A. Zargar, M Arora, T. Alshahrani, M. Shkir, Screen printed novel ZnO/MWCNTs nanocomposite thick films, Ceram Inter. 47(5) (2020) 6084-6093. https://doi.org/10.1016/j.ceramint.2020.10.185

S. Gea, C. T. Reynolds, N. Roohpour, B. Wirjosentono, N. Soykeabkaew, E. Bilotti, T. Peijs, Investigation into the structural, morphological, mechanical and thermal behaviour of bacterial cellulose after a two-step purification process, Biores. Technol. 102(19) (2011) 9105-9110, https://doi.org/10.1016/j.biortech.2011.04.077

S. I. Siddiqui, S. A. Chaudhry, Nanohybrid composite Fe_2O3-ZrO_2/BC for inhibiting the growth of bacteria and adsorptive removal of arsenic and dyes from water, J. Clean. Prod. 223 (2019) 849-868. https://doi.org/10.1016/j.jclepro.2019.03.161

S. I. Siddiqui, F. Zohra, S. A. Chaudhry, Nigella sativa seed based nanohybrid composite-Fe_2O_3-SnO_2/BC: a novel material for enhanced adsorptive removal of methylene blue from water, Environ. Res. 178 (2019) 108667. https://doi.org/10.1016/j.envres.2019.108667

S. Li, M. Zhang, Y. Gao, B. Bao, S. Wang, ZnO-Zn/CNT hybrid film as light-free nanocatalyst for degradation reaction, Nano Energy 2(6) (2013) 1329-1336. https://doi.org/10.1016/j.nanoen.2013.06.015

V. N. An, T. T. T. Van, H. T. C. Nhan, L.V. Hieu, Investigating methylene blue adsorption and photocatalytic activity of ZnO/CNC nanohybrids, J. Nanomat. (2020) 6185976. https://doi.org/10.1155/2020/6185976

Y. D. Dong, H. Zhang, G. J. Zhong, G. Yao, B. Lai, Cellulose/carbon composites and their applications in water treatment - a review, Chem. Eng. J. 405 (2021) 126980. https://doi.org/10.1016/j.cej.2020.126980

Y. Sun, J.H Seo, C. J. Takacs, J. Seifter, A. J. Heeger, Inverted polymer solar cells integrated with a low-temperature-annealed sol-gel-derived ZnO film as an electron transport layer, Adv. Mater. 23 (14) (2011) 1679-1683. https://doi.org/10.1002/adma.201004301

Y. Sun, S. R. Wilson, D. I. Schuster, High dissolution and strong light emission of carbon nanotubes in aromatic amine solvents, J. Am. Chem. Soc. 123 (2001) 5348-5349. https://doi.org/10.1021/ja0041730

Y. W. Koh, M. Lin, C. K. Tan, Y. L. Foo, K. P. Loh, Self-assembly and selected area growth of zinc oxide nanorods on any surface promoted by an aluminum precoat, J. Phys. Chem. B. 108(31) (2004) 11419-11425. https://doi.org/10.1021/jp049134f